Transmission of Magnetic Interactions through an Organometallic Coupler: A Novel Family of Metallocene-Substituted α-Nitronyl Aminoxyl Radicals

O. Jürgens,[†] J. Vidal-Gancedo,[†] C. Rovira,[†] K. Wurst,[‡] C. Sporer,[‡] B. Bildstein,[‡] H. Schottenberger,[‡] P. Jaitner,*[,‡] and J. Veciana*[,†]

Institut de Ciència de Materials de Barcelona (CSIC), Campus Universitari UAB, 08193 Bellaterra, Spain, and Institut für Allgemeine, Anorganische und Theoretische Chemie, Universität Innsbruck, Innrain 52a, A-6020, Innsbruck, Austria

Received May 4, 1998

The capability of metallocene bridges as new organometallic magnetic couplers is evaluated by studying the family of diradicals **2** (M = Fe, Ru) consisting of two purely organic α-nitronyl aminoxyl radicals connected by a 1,1′-metallocenylene bridge. Preliminary studies performed with 2-metallocenyl-α-nitronyl aminoxyl monoradicals **1** (M = Fe, Ru, Os), as reference compounds, show the presence of a small spin density on the central metal of the metallocenes. This fact makes the metallocene units effective bridges to transmit magnetic interactions by a spin polarization mechanism. The study of the magnetic properties of diradicals **2** in the solid state and in diluted frozen solutions reveals the existence of an intramolecular antiferromagnetic exchange interaction between the radical subunits whose strength is highly dependent on the molecular conformation adopted by the diradical. As shown by crystal data and by ESR measurements, an intramolecular hydrogen bond between the two radical units forces the molecule to adopt a *cisoid* molecular conformation, which determines that the magnetic interaction occurs by a direct through-space interaction between the two SOMOs of the two radical units along with the classical spin polarization mechanism through the σ-bonds of the metallocene unit. Lattice constants for both structures are as follows: **1** (M = Fe), $C_{17}H_{21}FeN_2O_2$, $a = 7.170(1)$ Å, $b = 10.135(2)$ Å, $c = 10.683(2)$ Å, $\alpha = 88.88(3)°$, $\beta = 83.42(3)°$, $\gamma = 79.75(3)°$, triclinic, $P\bar{1}$, $Z = 2$; **2** (M = Fe), $C_{24}H_{32}FeN_4O_4$, $a = 11.848(3)$ Å, $b = 11.785(2)$ Å, $c = 17.728(4)$ Å, $\beta = 106.25(2)°$, monoclinic, $P2_1/n$, $Z = 4$.

Introduction

One of the general approaches to high-spin organic compounds is based on conjugated polyradicals with topologically polarized π-spins.[1] These compounds are designed using an appropriate ferromagnetic coupling unit able to align in parallel the electron spins of a pair (or triad) of radical centers connected through such a unit.[2] *m*-Phenylene has become the most widely used ferromagnetic coupler because it is highly dependable.[1] Thus, this unit is able to couple ferromagnetically not only carbon- and nitrogen-centered free radicals but also carbenes, nitrenes, and polarons.[3] In addition, *m*-phenylene couplers can be modified with a large variety of substituents without changing the robust spin preference dictated by the topology rules,[4] except for few cases where a large torsion angle between the nodal plane of the π-spin source and the coupler unit plane is induced.[5] This result can be attributed to the electronic interaction through the σ-bond of the coupler unit that becomes significant for tilted π-systems.[6] Along with *m*-phenylene, several other purely organic units, including heteroatomic and hydrocarbon cycles, have been shown to be robust ferromagnetic couplers.[7]

In view of the central role played by the ferromagnetic coupling units in the design of magnetic materials, the development and study of new ferromagnetic couplers is important. The use of metalloorganic spacers, like metallocenes, as magnetic couplers of radical centers covalently linked to them was unprecedented. In fact, metallocenes had only been used as building blocks of molecular solids promoting intermolecular magnetic exchange interactions very successfully.[1c] So, we

* Prof. Jaume Veciana is the author to whom correspondence should be addressed (phone, +(34)-3-5801853; fax, +(34)-3-5805729; e-mail, VECIANAJ@icmab.es).

[†] Institut de Ciència de Materials de Barcelona.

[‡] Universität Innsbruck.

(1) (a) Gateschi, D.; Kahn, O.; Miller, S.; Palacio, F. *Molecular Magnetic Materials*; Kluwer Academic: Dordrecht, 1991. (b) Kahn, O. *Molecular Magnetism*; VCH Publishers: Weinheim, 1993. (c) Miller, J. S.; Epstein, A. J. *Angew. Chem., Int. Ed. Engl.* **1994**, *33*, 385. (d) Rajca, A. *Chem. Rev.* **1994**, *94*, 871−893.

(2) (a) Mataga, N. *Theor. Chim. Acta* **1968**, *10*, 372. (b) Borden, W. T., Ed. *Diradicals*; Wiley: New York, 1982. (c) Iwamura, H. *Adv. Phys. Org. Chem.* **1990**, *26*, 179−253. (d) Dougherty, D. A. *Acc. Chem. Res.* **1991**, *24*, 88.

(3) For selected examples of the use of *m*-phenylene as a ferromagnetic coupler, see: Schlenk, W.: Braum, M. *Ber. Dtsch. Chem. Ges.* **1915**, *48*, 661. Kothe, G.; Denke, K.-H.; Sümmermann, W. *Angew. Chem., Int. Ed. Engl.* **1970**, *9*, 906−907. Calder, A.; Forrester, A. R.; James, P. G.; Luckhurst, G. R. *J. Am. Chem. Soc.* **1969**, *91*, 3724−3727. Ishida, T.; Iwamura, H. *J. Am. Chem. Soc.* **1991**, *113*, 4238. Dougherty, D. A. *Mol. Cryst. Liq. Cryst.* **1989**, *176*, 25. Wassermann, E.; Murray, R. W.; Yager, W. A.; Trogollo, A. M.; Smolinsky, G. *J. Am. Chem. Soc.* **1967**, *89*, 5076. Tukada, H.; Mutai, K.; Iwamura, H. *J. Chem. Soc., Chem. Commun.* **1987**, 1159.

(4) Kasai, D. A.; Chang, W.; Dougherty, D. A. *J. Am. Chem. Soc.* **1991**, *113*, 2764. Rajca, A. *J. Am. Chem. Soc.* **1990**, *112*, 5890. Rajca, A.; Utamapanya, S.; Xu, J. *J. Am. Chem. Soc.* **1991**, *113*, 9235. Veciana, J.; Rovira, C.; Armet, O.; Domingo, V. M.; Crespo, M. I.; Palacio, F. *J. Am. Chem. Soc.* **1991**, *113*, 2552−2561.

(5) Borden, W. T.; Iwamura, H.; Berson, J. A. *Acc. Chem. Res.* **1994**, *27*, 109−116. Dvolaitzky, M.; Chiarelly, R.; Rassat, A. *Angew. Chem., Int. Ed. Engl.* **1992**, *31*, 180−181. Kanno, F.; Inone, K.; Kago, N.; Iwamura, H. *J. Am. Chem. Soc.* **1993**, *115*, 847−850.

(6) Fang, S.; Lee, M.-S.; Hrovat, D. A.; Borden, W. T. *J. Am. Chem. Soc.* **1995**, *117*, 6727−6731.

(7) West, A. P., Jr.; Silverman, S. K.; Dougherty, D. A. *J. Am. Chem. Soc.* **1996**, *118*, 1452−1463 and references therein.

S0020-1669(98)00495-9 CCC: $15.00
Published on Web 08/13/1998

addressed our attention to diradicals having two radical centers connected through 1,1′-metallocenylene units in order to evaluate their ability as spin couplers. As organic radicals we chose 4,4,5,5-tetramethyl-4,5-dihydro-1*H*-imidazol-3-oxide-1-yl oxyl radicals, hereafter named as α-nitronyl aminoxyl radicals, because of the synthetic availability of their precursors, the deep knowledge of their electronic and molecular structures, and also their large persistence.[1a] The particular structure of such diradicals makes them also interesting in order to test if a direct through-space interaction, mimicking a superexchange interaction,[1b] between the π-spins of the two radical centers and the metal orbitals of the metallocene would be possible.

We report here the synthesis and study of the series of monoradicals **1** (M = Fe, Ru, Os), as model compounds,[8] and diradicals **2** (M = Fe, Ru). The model compounds provided the opportunity to study the role played by the central metal in their electronic structure while the diradicals afforded insights about the magnetic interaction of radical centers which were found to be unfortunately antiferromagnetic and very sensitive to the molecular conformation.

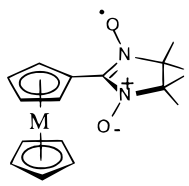

1 (M = Fe, Ru, Os)

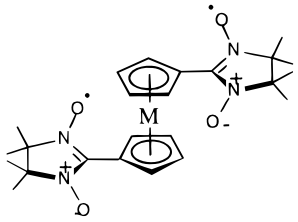

2 (M = Fe, Ru)

Experimental Section

General Procedures. All reactions were carried out under Ar using standard Schlenk techniques. Freshly distilled dry solvents were used throughout and were obtained following standard literature methods. Commercially available reagents were used as received. Infrared spectra were recorded with a Nicolet 510M FT-IR spectrometer. EI and FAB mass spectra were recorded on a Varian C7 and a Finnigan MAT spectrometer, respectively. UV/vis/near-IR spectra were recorded with a Varian Cary 5 spectrometer. Reference compounds 4,4,5,5-tetramethyl-3-oxide-imidazoline-1-oxyl monoradical[9] (HNN; **5**) and 4,4,5,5-tetramethyl-3-oxide-2-phenyl-imidazoline-1-oxyl monoradical[10] (PHNN; **6**) were synthesized as reported previously.

Magnetic Measurements. DC magnetic susceptibility data from 2 to 300 K, in magnetic fields of 0.5−1.0 T, were collected using a Quantum Design MPMS superconducting SQUID susceptometer and using microcrystalline samples (5−20 mg) of the radicals. The diamagnetic contributions of the sample holder and of the radicals, as well as the temperature-independent paramagnetism for radical **1** (M = Ru), were determined by extrapolation from the χT vs T plots in the high-temperature range and were used later to correct the SQUID outputs.

X-ray Measurements. X-ray data of single crystals of **1** (M = Fe) and **2** (M = Fe) were collected at 188 and 213 K, respectively, on a Siemens P4 diffractometer working with monochromatic Mo Kα (λ = 0.71073 Å) radiation. Data were collected via ω scans and corrected for Lorentz and polarization effects but not for absorption. The structures were all refined by a full-matrix least-squares method which minimized $\sum w(\Delta F)^2$. Atomic coordinates and other related structural data have been deposited as Supporting information.

ESR Spectroscopic Measurements. ESR spectra were recorded on a Bruker ESP-300E spectrometer operating in the X-band (9.3 GHz) with a rectangular TE102 cavity and equipped with a field-frequency (F/F) lock accessory and a built-in Bruker NMR gaussmeter ER 035 M. Signal-to-noise ratio was increased by accumulation of scans using the F/F lock accessory to guarantee a high-field reproducibility. Precautions to avoid undesirable spectral line broadening such as that arising from microwave power saturation and magnetic field overmodulation were taken. To avoid dipolar broadening, the radical solutions were carefully degassed three times using vacuum cycles with pure Ar. The spectrometer was equipped either with a Bruker ER 4121 HT nitrogen cryostat (100−300 K) or with a flowing-helium Oxford ESR-900 cryostat (4.2−300 K) controlled by an Oxford ITC4 temperature control unit with a custom-made double temperature control system for determining the sample temperature. Computer simulations of experimental spectra were carried out with the WINEPR Simfonia program.

Calculation of Zero Field Splitting Parameters. The program used was based on a model of localized electrons split into several fractions that was previously developed for bisnitroxide diradicals.[11] The following assumptions were made in these calculations. First, the spin-density distribution on each radical subunit was assumed to be +2/7 on the N and O atoms and −1/7 on the α-carbon atom, paralleling the calculated values for such radicals.[12] Second, the internal geometry of the two radical units and that of the metallocene unit were assumed to be the same as in the crystal structure of **2** (M = Fe) (similar to other metallocene derivatives).[13] Consequently, the molecular conformation of the diradical is determined just by the three dihedral angles ϕ_1, ϕ_2, and φ, which are defined in the description of the crystal structure of **2** (M = Fe).

Cyclic Voltammetry. Anhydrous acetonitrile was freshly distilled over P_2O_5 under nitrogen. Commercial tetrabutylammonium hexafluorophosphate (Fluka, electochemical grade) was used as supporting electrolyte. A platinum spiral was used as the working electrode, a platinum thread as the counter electrode, and a Ag/AgCl electrode as the reference electrode. Deoxygenation of the solutions was achieved by saturation with Ar. All of the half-wave potentials are referred to Ag/AgCl. The cyclic voltammetries were carried out on a EG&G Instruments potentiostat/galvanostat, model 263A.

Preparation of Radical Derivatives. 4,4,5,5-Tetramethyl-3-oxide-2-ferrocenyl-imidazoline-1-oxyl Radical (1, M = Fe). Ferrocene carboxaldehyde (1.09 g; 5 mmol)[14] (**3**, M = Fe) and 1.23 g (5 mmol) of 2,3-dimethyl-2,3-bis(hydroxylammonium)butane sulfate[15] were refluxed in 80 mL of dry methanol for 1 h. After the initial orange suspension became red and clear, the solution was cooled to room temperature and 1.12 g *t*-BuOK was added. The mixture was stirred for 15 min at room temperature and then cooled to 0 °C for an additional 2 h until an abundant precipitate was observed. The suspension was filtered and evaporated, the residue was dissolved in 80 mL toluene, and 8 g of PbO_2 was added. This suspension was stirred for 12 h and then filtered, and the resulting deeply green solution was evaporated and chromatographed on SiO_2 eluting with diethyl ether. Dark brown microcrystals (570 mg) of radical **1** (M = Fe) were obtained (yield: 35%). IR (KBr): ν 1361, 1203, 1107, 1004 cm^{-1}. UV/vis: λ_{max} (log ϵ) 294 (4.1), 315 (4.0), 368 (3.9), 463 (2.8), 638 (2.9), 685 (2.9) nm. MS (EI): *m*/*e* 342, 341 (M^+), 325, 310, 211. Anal. Found: C, 60.34; H, 6.39; N, 8.01. Calcd for $C_{17}H_{21}N_2O_2Fe$: C, 59.83; H, 6.20; N, 8.20.

(8) Monoradical **1** (M = Fe) was synthesized some time ago, and its magnetic solid state properties were studied. See: (a) Owtscharenko, W.; Huber, W.; Schwarzhans, K. E. *Z. Naturforsch.* **1986**, *41b*, 1587−1588. (b) Nakamura, Y.; Koga, N.; Iwamura, H. *Chem. Lett.* **1991**, 69−72. Nevertheless, the spin density distribution of this monoradical was not studied in detail by such authors.

(9) Hosokoshi, Y.; Tamura, M.; Nozawa, K.; Suzuki, S.; Kinoshita, M.; Sawa, H.; Kato R. *Synth. Met.* **1995**, *71*, 1795−1796.

(10) Ullman, E. F.; Osiecki, J. H.; Boocock, D. G. B.; Darcy, R. *J. Am. Chem. Soc.* **1972**, *94*, 7049. D'Anna, J. A.; Wharton, J. N. *J. Chem. Phys.* **1970**, *53*, 4047. Veciana, J.; Cirujeda, J.; Rovira, C.; Vidal-Gancedo, J. *Adv. Mater.* **1995**, *7*, 221.

(11) Michon, J.; Michon, P.; Rassat, A. *Nouv. J. Chim.* **1980**, *4*, 523−526.

(12) Cirujeda, J. Ph.D. Thesis, Universitat Ramon Llull, Barcelona, 1997.

(13) Seiler, P.; Dunitz, D. *Acta Crystallogr., Sect. B* **1980**, *36*, 2946−2950.

(14) Balavoine, G. G. A.; Doisneau, G.; Fillebeen-Khan, T. *J. Organomet. Chem.* **1991**, *412*, 381−382.

(15) Lamchen, M.; Mittag, T. W. *J. Chem. Soc.* **1996**, 2300−2303.

Scheme 1

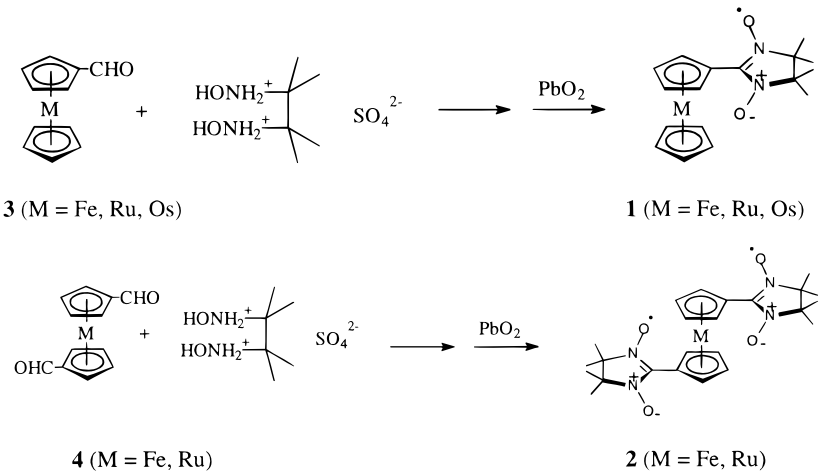

3 (M = Fe, Ru, Os) **1** (M = Fe, Ru, Os)

4 (M = Fe, Ru) **2** (M = Fe, Ru)

4,4,5,5-Tetramethyl-3-oxide-2-ruthenocenyl-imidazoline-1-oxyl Radical (1, M = Ru). Preparation followed the same procedure as for **1** (M = Fe). The oxidation time was 4 h in this case. From 50 mg of ruthenocene carboxaldehyde[16,17] (**3**, M = Ru) was obtained 24 mg of blue microcrystals of radical **1** (M = Ru) (yield: 32%). IR (KBr): ν 1365, 1203, 1103, 1028 cm^{-1}. UV/vis: λ_{max} (log ϵ) 263 (4.1), 346 (4.0), 604 (1.5), 661 (2.9) nm. MS (EI): *m*/*e* 387, 386 (M$^+$), 256. MS (FAB): *m*/*e* 387, 371, 256. Anal. Found: C, 53.20; H, 5.61; N, 7.02. Calcd for $C_{17}H_{21}N_2O_2Ru$: C, 52.83; H, 5.47; N, 7.24.

4,4,5,5-Tetramethyl-3-oxide-2-osmocenyl-imidazoline-1-oxyl radical (1, M = Os). Preparation was analogous to **1** (M = Fe) using an oxidation time of 1 h. From 50 mg of osmocene carboxaldehyde[16,17] (**3**, M = Os) was obtained 22 mg of sky blue crystals of radical **1** (M = Os) (yield: 32%). IR (KBr): ν 1364, 1202, 1099, 1024 cm^{-1}. UV/vis: λ_{max} (log ϵ) 246 (3.7), 342 (3.8), 604 (2.6), 657 (2.7) nm. MS (EI): *m*/*e* 476, 475 (M$^+$), 345. Anal. Found: C, 43.09; H, 4.59. Calcd for $C_{17}H_{21}N_2O_2Os$: C, 42.93; H, 4.44.

2,2′-Di-(1,1′-ferrocenediyl)-4,4,5,5-tetramethyl-4,5-dihydro-1*H*-imidazol-3-oxide-1-yl Oxyl Diradical (2, M = Fe). 2,3-Dimethyl-2,3-bis(hydroxylammonium)butane sulfate (2.24 g; 9.09 mmol) and 2.06 g (18.4 mmol) of *t*-BuOK were suspended in 20 mL of EtOH, sonicated for 10 min in an ultrasound bath, and stirred for 30 min at 50 °C. Then 1,1′-ferrocene dicarboxaldehyde[14] (**4**, M = Fe) (1 g, 4.13 mmol) was added. The resulting solution was sonicated again for 15 min and finally stirred for another 2 h at 50 °C. The solution was evaporated and the residue suspended in 20 mL of toluene, to which an excess of PbO_2 (6 g, 25.1 mmol) was added, and the resulting suspension was stirred for 1−2 h. As soon as the solution did not show any further change (TLC control), the suspension was filtered and the filtrate solution evaporated and chromatographed on SiO_2 eluting with diethyl ether. Deep green microcrystals (120 mg) of diradical **2** (M = Fe) were obtained (yield: 7%). IR (KBr): ν 1416, 1387, 1366, 1202, 1163, 1140, 1034 cm^{-1}. UV/vis: λ_{max} (log ϵ) 228 (4.3), 314 (4.3), 371 (3.9), 477 (3.0), 637 (3.1), 686 (3.1) nm. MS (EI): *m*/*e* 496.5 (M$^+$), 480.5, 464.5, 366, 278, 268, 252, 236. Anal. Found: C, 57.77; H, 6.49; N, 10.98. Calcd for $C_{24}H_{32}N_4O_4Fe$: C, 58.06; H, 6.70; N, 11.28.

2,2′-Di-(1,1′-ruthenocenediyl)-4,4,5,5-tetramethyl-4,5-dihydro-1*H*-imidazol-3-oxide-1-yl Oxyl Diradical (2, M = Ru). 2,3-Dimethyl-2,3-bis(hydroxylammonium)butane sulfate (151 mg; 0.613 mmol) and 80 mg (0.278 mmol) of 1,1′-ruthenocene dicarboxaldehyde[16,17] (**4**, M = Ru) were dissolved in 10 mL of MeOH and sonicated for 5 min, and the resulting solution was refluxed for 1 h and left to cool to room temperature. Then, 141 mg (1.25 mmol) *t*-BuOK was added to the solution and it was stirred for another 2 h at 0 °C. The resulting yellow-reddish solution was filtered and evaporated under Ar. The residue was suspended in 20 mL of toluene, and 1.50 g (6.3 mmol) PbO_2 was added. Vigorous stirring was continued for 2 h. The suspension was filtered and the filtrate solution evaporated and chromatographed on SiO_2 eluting with diethyl ether. Deep blue crystals (30 mg) of diradical **2** (M = Ru) were obtained (yield: 20%). IR (KBr): ν 1412, 1385, 1369, 1202, 1140, 1101, 1032, 1022 cm^{-1}. UV/vis: λ_{max} (log ϵ) 227 (4.2), 263 (4.3), 348 (4.3), 602 (3.3), 656 (3.3) nm. MS (EI): *m*/*e* 542 (M$^+$), 526, 510, 412, 234, 219, 197, 167. Anal. Found: C, 53.71; H, 6.31; N, 10.04. Calcd for $C_{24}H_{32}N_4O_4Ru$: C, 53.22; H, 5.96; N, 10.34.

Results and Discussion

Synthesis of Radical Derivatives. Synthetic routes for preparing radical derivatives are summarized in Scheme 1. Radicals **1** (M = Fe, Ru, Os) were obtained from the metallocene carboxaldehyde precursors **3** (M = Fe, Ru, Os) by condensation with 2,3-dimethyl-2,3-bis(hydroxylammonium)-butane sulfate and further oxidation with PbO_2. Diradicals **2** (M = Fe, Ru) were synthesized analogously from the corresponding 1,1′-metallocene dicarboxaldehyde precursors **4** (M = Fe, Ru). Osmocene and ruthenocene,[18,19] as well as the carboxaldehyde **3** (M = Fe, Ru, Os) and 1,1′-dicarboxaldehyde derivatives **4** (M = Fe, Ru), were synthesized following standard synthetic methods.[14−17]

Solid State Structures. General crystallographic data for radical **1** (M = Fe) and diradical **2** (M = Fe) are summarized in Table 1.

Radical **1** (M = Fe) crystallizes in the triclinic $P\bar{1}$ space group with an asymmetric unit containing one radical molecule. Table 2 lists atomic coordinates for **1** (M = Fe). Figure 1a shows its solid state molecular conformation along with the atom-numbering scheme.

The most relevant conformational features of this radical are (a) the small torsion angle of 9° between the imidazoline and the cyclopentadienyl (Cp) rings and (b) the eclipsed arrangement of the two Cp rings of the metallocene unit. This kind of eclipsed arrangement is the normal one observed for substituted linear metallocenes.[20] In the same way the average Fe−C distance of 2.047 Å and the distance from the iron atom to the two Cp ligands (1.641 and 1.639 Å) are the normal ones [2.045-(1) and 1.65 Å, respectively] for most ferrocene derivatives.[21]

(16) Sanders, R.; Mueller-Westerhoff, U. T. *J. Organomet. Chem.* **1996**, *463*, 163−167.
(17) Mueller-Westerhoff, U. T.; Yang, Z.; Ingram, G. *J. Organomet. Chem.* **1993**, *463*, 163−167.
(18) Ingram, G.; Jaitner, P.; Schwarzhans, K. E. *Z. Naturforsch.* **1990**, *45b*, 781−784.
(19) Pertici, P.; Vitulli, G.; Paci, M.; Porri, P. *J. Chem. Soc., Dalton. Trans.* **1980**, 1961.
(20) Doman, T. N.; Landis, C. R.; Bosnich, B. *J. Am. Chem. Soc.* **1992**, *114*, 7264−7272.
(21) Seiler, P.; Dunitz, J. D. *Acta Crystallogr., Sect. B* **1979**, *35*, 1068.

Table 1. Crystallographic Data for Radical **1** (M = Fe) and Diradical **2** (M = Fe)[a]

compd	**1** (M = Fe)	**2** (M = Fe)
formula	$C_{17}H_{21}FeN_2O_2$	$C_{24}H_{32}FeN_4O_4$
a (Å)	7.170(1)	11.848(3)
b (Å)	10.135(2)	11.785(2)
c (Å)	10.683(2)	17.728(4)
α (deg)	88.88(3)	90
β (deg)	83.42(3)	106.25(2)
γ (deg)	79.75(3)	90
V (Å$^{3)}$	758.9(2)	2376.4(9)
Z	2	4
fw (g/mol)	341.21	496.39
space group	$P\bar{1}$ (No. 2)	$P2_1/n$ (No. 14)
T (K)	188(2)	213(2)
λ (Å)	0.710 73	0.710 73
ρ_{calcd} (g cm^{-3})	1.493	1.387
μ (cm^{-1})	10.02	6.72
R (F_o)[b]	0.0314	0.0488
R_w (F_o)[b]	0.0377	0.0876

[a] ESDs refer to the last digit printed. [b] $R = \sum||F_o| - |F_c||/\sum|F_o|$. $R_w = [\sum w(||F_o| - |F_c||)^2/(\sum w|F_o|^2)]^{1/2}$.

Table 2. Atomic Coordinates and Equivalent Isotropic Displacement Parameters for Non-hydrogen Atoms of **1** (M = Fe)[a]

	x	y	z	U_{eq},[b] Å^2
Fe1	0.1060(1)	0.5398(1)	0.2450(1)	0.020(1)
O1	−0.2610(4)	0.8350(2)	0.0455(2)	0.035(1)
O2	−0.1670(4)	0.8432(2)	0.4674(2)	0.031(1)
N1	−0.2502(4)	0.8766(3)	0.1567(2)	0.021(1)
N2	−0.2026(4)	0.8806(3)	0.3558(2)	0.019(1)
C1	−0.2040(4)	0.7983(3)	0.2576(3)	0.018(1)
C2	−0.2133(5)	1.0238(3)	0.3129(3)	0.020(1)
C3	−0.3163(4)	1.0209(3)	0.1942(3)	0.019(1)
C4	−0.1616(16)	0.6552(14)	0.2603(8)	0.020(2)
C5	−0.1347(14)	0.5660(9)	0.1535(7)	0.028(2)
C6	−0.0886(14)	0.4313(10)	0.1944(9)	0.034(2)
C7	−0.0898(12)	0.4340(8)	0.3288(8)	0.027(2)
C8	−0.1345(11)	0.5687(9)	0.3713(6)	0.025(2)
C9	0.3068(17)	0.6630(15)	0.2236(10)	0.042(2)
C10	0.3252(13)	0.5743(11)	0.1178(8)	0.038(2)
C11	0.3607(13)	0.4388(11)	0.1611(9)	0.036(2)
C12	0.3617(13)	0.4438(11)	0.2955(9)	0.042(2)
C13	0.3264(14)	0.5766(12)	0.3321(9)	0.046(2)
C21	−0.0054(6)	1.0443(4)	0.2845(4)	0.027(1)
C22	−0.3170(5)	1.1201(3)	0.4163(3)	0.026(1)
C31	−0.2614(5)	1.1144(3)	0.0884(3)	0.028(1)
C32	−0.5338(6)	1.0408(4)	0.2212(5)	0.028(1)

[a] ESDs refer to the last digit printed. [b] U_{eq} is one-third of the trace of the orthogonalized $\boldsymbol{U}_{ij}$ tensor.

The crystal packing of radical **1** (M = Fe) (Figure 1b) seems to be determined by weak intermolecular C−H···O hydrogen bonds.[22] Molecules are paired forming dimers by means of two complementary C_{methyl}−H21···O2^i−N2^i hydrogen bonds [i = 2 − x, 2 − y, 1 − z; d(H21···O2^i) = 2.54 Å; θ(C21−H21···O2^i) = 139°]. These dimers are linked to each other, forming chains along the crystallographic [101] direction by means of another C_{methyl}−H32B···O1^{ii}−N1^{ii} hydrogen bond [ii = 1 − x, 2 − y, − z; d(H32B···O1^{ii}) = 2.70 Å; θ(C32−H32B···O1^{ii}) = 136°]. As will be discussed later, such dimers are relevant for the solid state magnetic properties of this compound.

Diradical **2** (M = Fe) crystallizes in the monoclinic $P2_1/n$ space group with an asymmetric unit containing one diradical molecule. Table 3 lists atomic coordinates for **2** (M = Fe). Figure 2a shows its solid state molecular conformation together with the atom-numbering scheme.

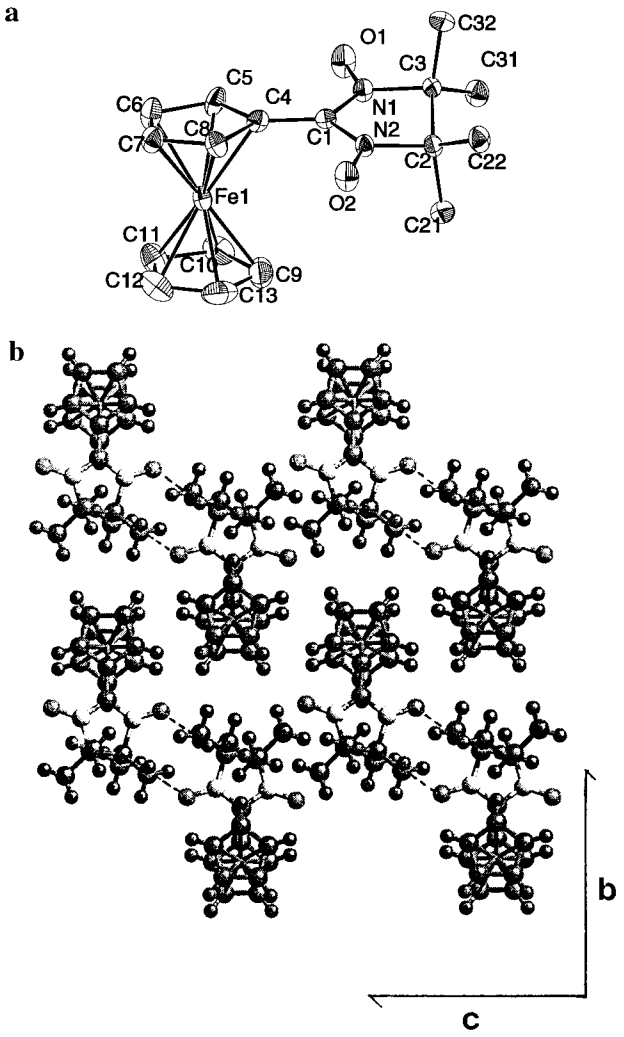

Figure 1. (a) Atomic numbering scheme and molecular conformation of monoradical **1** (M = Fe) with thermal vibrational ellpsoids (50%). (b) Crystal packing of monoradical **1** (M = Fe) projected on the crystallographic plane (100) showing that the dimers are connected by means of C_{methyl}−H21···O2^i−N2^i hydrogen bonds [i = 2 − x, 2 − y, 1 − z].

The molecular conformation of this diradical has several interesting points that deserve to be discussed. Surprisingly, only one imidazoline ring of diradical **2** keeps planarity with respect to its adjacent cyclopentadienyl ring with a dihedral angle ϕ_1 of 7° between the mean planes of both rings, while the other imidazoline ring is tilted by an angle ϕ_2 of 24°. The average Fe−C distance (2.047 Å) and the Fe−Cp distance (1.652 Å) of **2** (M = Fe) are the normal ones expected for a substituted ferrocene.[20,21] The two Cp rings are also eclipsed, although, unusually, the relative arrangement of the two substituents on the cyclopentadienyl rings is not in a *transoid* conformation, as would normally be expected for 1,1′-disubstituted metallocenes bearing conjugated substituents,[23,24] but in a *cisoid* one. Hence, the dihedral angle φ formed by the atoms C6 and C06, which connect the imidazoline rings to the ferrocene, and the centroids of the two Cp rings of the ferrocene unit is 73°. All of the above-mentioned conformational facts can be conveniently rationalized by the existence of an intramolecular hydrogen bond between one methyl group of one

(22) Taylor, R.; Kennard, O. *J. Am. Chem. Soc.* **1982**, *104*, 5063.

(23) Moore, A. J.; Skabara, P. J.; Bryce, M. R.; Batsanov, A. S.; Howard, J. A. K.; Daley, S. T. A. K. *J. Chem. Soc., Chem. Commun.* **1993**, 413−419.

(24) Gelin, F.; Thummel, R. P. *J. Org. Chem.* **1992**, *57*, 3780−3783.

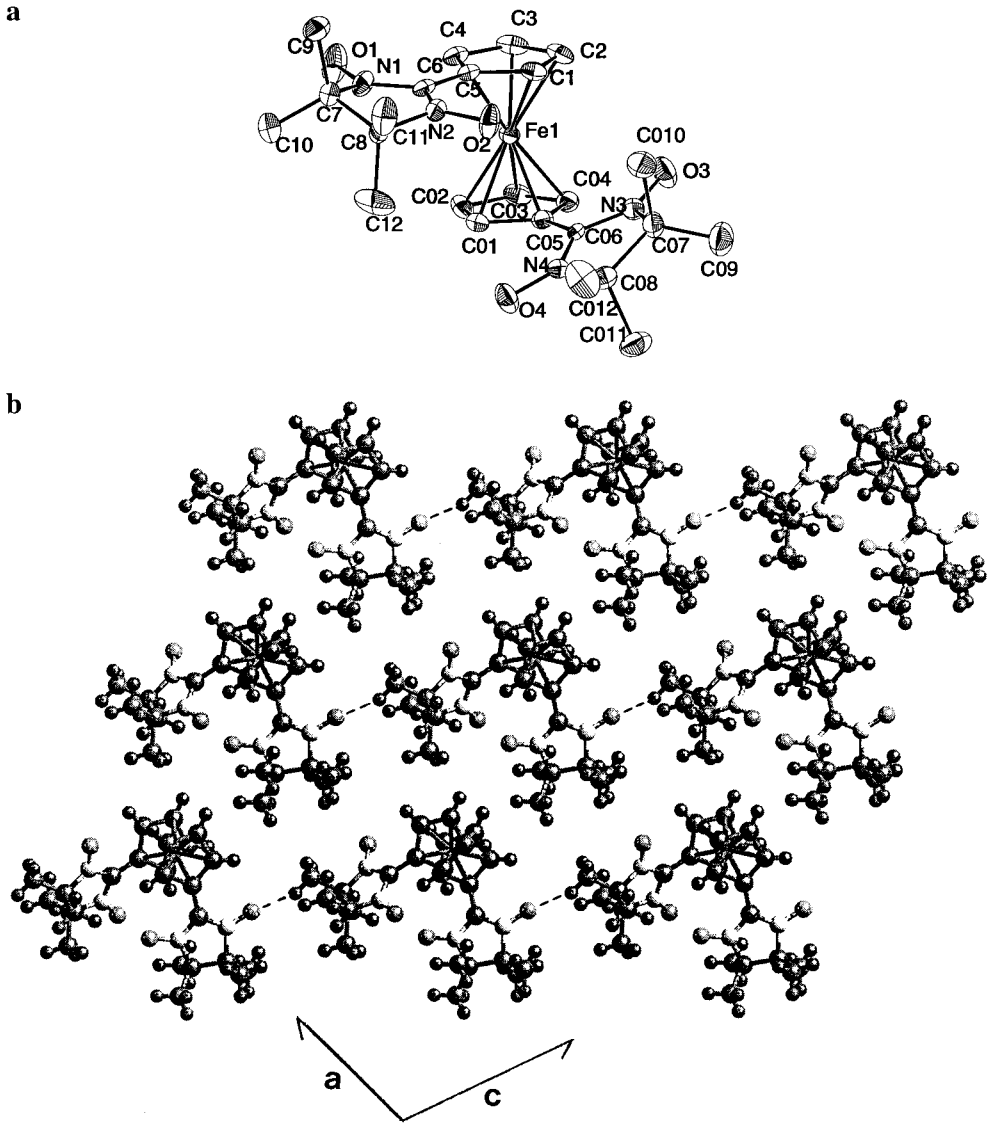

Figure 2. (a) Atomic numbering scheme and molecular conformation of diradical **2** (M = Fe) with thermal vibrational ellpsoids (50%). (b) Crystal packing of diradical **2** (M = Fe) projected on the crystallographic plane (010). In this view are shown chains of molecules connected through C_{methyl}−H09C···O1^{i}−N1^{i} hydrogen bonds [$i = x - {}^1/_2, -y - {}^1/_2, z + {}^1/_2$] (dashed lines) along the crystallographic [10$\bar{1}$] direction.

radical subunit and one of the two N−O groups of the other radical subunit, C010−H01A···O2−N2 [d(H01A···O2) = 2.48 Å; θ(C010−H01A···O2) = 172°], which forces both radical subunits of the ferrocene to keep close to each other. Therefore this compound is a new, rare example of a *cisoid* conformation in a 1,1′-disubstituted metallocene which can be rationalized by the existence of an intramolecular attractive interaction between the 1,1′-substituents.[25] The crystal packing of diradical **2** (M = Fe) (Figure 2b) is also apparently controlled by the C_{methyl}−H09C···O1^{i}−N1^{i} hydrogen bond [$i = x - {}^1/_2, -y - {}^1/_2, z + {}^1/_2$; d(H09C···O1^{i}) = 2.31 Å; θ(C09−H09C···O1^{i}) = 144°]. These hydrogen bonds arrange the molecules into chains along the crystallographic [10$\bar{1}$] direction, the chains being arranged into planes perpendicular to the [010] direction by means of other weak interactions. Table 4 summarizes the most relevant structural parameters for **1** (M = Fe) and **2** (M = Fe).

Electronic Structure of Metallocene Radicals. The electronic structures of radicals **1** (M = Fe, Ru, Os) and diradicals **2** (M = Fe, Ru) were first studied by electronic absorption spectroscopy. Table 5 summarizes the resulting spectral data.

The spectrum of **1** (M = Fe) has two weak absorption maxima in the visible range at 638 and 685 nm, which typically appear for conjugated α-nitronyl aminoxyl radicals in apolar solvents between 600 and 650 nm.[10] Other intense absorptions are observed at 294, 315, and 368 nm which also correspond to other electronic transitions of the α-nitronyl aminoxyl moiety. On the other hand, the absorption maximum appearing at 463 nm can be ascribed to the forbidden 3d−3d transition of the ferrocene moiety.[26] In accord with the conjugation existing between the α-nitronyl aminoxyl and the ferrocene moiety, this band is shifted bathochromically and shows a hyperchromic effect with respect the corresponding band of unsubstituted ferrocene.[27] Thus, the molecule of radical **1** (M = Fe) shows only small modifications of the basic electronic features of the α-nitronyl aminoxyl and ferrocene units in isolation. The UV/vis spectra of **1** (M = Ru) and **1** (M = Os) are very similar to each other. They show the two typical bands (Table 5) of substituted α-nitronyl aminoxyl radicals.[10] However, there are

(25) Togni, A.; Hobi, M.; Rihs, G.; Rist, G.; Albinati, A.; Zanello, P.; Zech, D.; Keller, H. *Organometallics* **1994**, *13*, 1224−1234.

(26) (a) Gmelin *Handbuch der Anorganischen Chemie*, 3rd ed.; Springer: Berlin, 1974; Vol. 14, p 45. (b) Geoffroy, G. L.; Wrighton, M. S. *Organometallic Photochemistry*; Academic Press: New York, 1979; p 237.

(27) Lundquist, R. T.; Cais, M. *J. Org. Chem.* **1962**, *27*, 1167−1172.

Table 3. Atomic Coordinates and Equivalent Isotropic Displacement Parameters for Non-Hydrogen Atoms of **2** (M = Fe)[a]

	x	*y*	*z*	U_{eq},[b] Å^2
Fe1	0.6230(1)	0.2274(1)	0.7900(1)	0.025(1)
O1	0.9657(3)	0.2022(4)	0.7595(2)	0.063(1)
O2	0.8688(3)	0.1469(3)	0.9920(2)	0.048(1)
O3	0.4493(3)	0.1690(3)	0.9304(2)	0.051(1)
O4	0.7323(3)	0.4484(3)	1.0073(2)	0.048(1)
N1	0.9723(4)	0.1981(4)	0.8326(2)	0.035(1)
N2	0.9267(4)	0.1709(3)	0.9426(2)	0.030(1)
N3	0.5255(4)	0.2362(4)	0.9739(2)	0.033(1)
N4	0.6600(4)	0.3685(3)	1.0104(2)	0.029(1)
C1	0.6808(5)	0.0815(4)	0.8502(3)	0.031(1)
C2	0.5806(5)	0.0581(4)	0.7869(3)	0.037(1)
C3	0.6052(5)	0.0901(5)	0.7165(3)	0.041(2)
C4	0.7218(5)	0.1332(4)	0.7354(3)	0.033(1)
C5	0.7694(4)	0.1277(4)	0.8191(3)	0.026(1)
C6	0.8863(4)	0.1637(4)	0.8638(3)	0.026(1)
C7	1.0873(4)	0.2133(5)	0.8939(3)	0.033(1)
C8	1.0439(4)	0.2300(5)	0.9682(3)	0.031(1)
C9	1.1568(5)	0.1031(5)	0.8945(3)	0.048(2)
C10	1.1547(5)	0.3133(5)	0.8730(4)	0.052(2)
C11	1.1188(5)	0.1748(6)	1.0432(3)	0.054(2)
C12	1.0182(5)	0.3539(5)	0.9827(4)	0.054(2)
C01	0.6691(5)	0.3858(4)	0.8374(3)	0.029(1)
C02	0.6259(5)	0.3936(4)	0.7546(3)	0.037(2)
C03	0.5097(5)	0.3511(4)	0.7323(3)	0.036(1)
C04	0.4796(4)	0.3148(4)	0.7999(3)	0.031(1)
C05	0.5800(4)	0.3370(4)	0.8666(3)	0.027(1)
C06	0.5897(4)	0.3147(4)	0.9476(3)	0.024(1)
C07	0.5651(4)	0.2247(5)	1.0617(3)	0.036(1)
C08	0.6340(5)	0.3359(4)	1.0858(3)	0.032(1)
C09	0.4600(5)	0.2055(6)	1.0921(4)	0.059(2)
C010	0.6435(6)	0.1176(5)	1.0781(4)	0.053(2)
C011	0.5581(6)	0.4324(5)	1.1037(3)	0.056(2)
C012	0.7471(6)	0.3278(6)	1.1507(4)	0.066(2)

[a] ESDs refer to the last digit printed. [b] U_{eq} is one-third of the trace of the orthogonalized $\boldsymbol{U}_{ij}$ tensor.

Table 4. Selected Intra- and Intermolecular Distances (Å) and Angles (deg) for Monoradical **1** (M = Fe) and Diradical **2** (M = Fe)[a]

1 (M = Fe)		**2** (M = Fe)	
Fe−C[b]	2.047(10) Å	Fe−C[b]	2.047(5) Å
Fe−Cp[c]	1.639(9); 1.641(9) Å	Fe−Cp[c]	1.652(5) Å
Im, Cp[d]	9.0(5)°	Im, Cp[d]	7.0(5); 24.0(5)°
H21···O2[i]	2.54(1) Å	H01A···O2	2.48(1) Å
C21, H21, O2[i]	139.0(5)°	C010, H01A, O2	172.0(5)°
H32B···O1[ii]	2.70(1) Å	H09C···O1[i]	2.31(1) Å
C32, H32B, O1[ii]	136(1)°	C09, H09C, O1[i]	144(1)°

[a] See text for symmetry codes. ESDs refer to the last digit printed. [b] Mean distance between Fe and C atoms of cyclopentadienyl rings. [c] Mean distance between Fe atom and center of cyclopentadienyl ring. [d] Mean torsion angle between imidazoline and cyclopentadienyl rings.

no absorption maxima which can be directly ascribed to the metallocene moieties, since ruthenocene and osmocene are known to be transparent and practically do not absorb in the UV/vis region.[28] The absorption spectra of the biradicals **2** (M = Fe, Ru) are very similar to those of the corresponding monoradicals **1** (M = Fe, Ru) (Table 5), indicating that the electronic structure of the radical moieties in the diradicals is basically the same, regardless the introduction of a second α-nitronyl aminoxyl unit attached to the metallocene.

In conclusion, the electronic interactions among the metallocene units and the radical moieties in the monoradicals and diradicals are too weak to be observed by this technique. To gain more detailed information about these possible electronic interactions, cyclic voltammetry and electron spin resonance were used.

(28) (a) Wilkinson, G. *J. Am. Chem. Soc.* **1952**, *74*, 6146−6147. (b) Fischer, E. O.; Grubert, H. *Chem. Ber.* **1959**, *92*, 2302−2309.

Table 5. Absorption Maxima, λ_i in nm, of Radicals **1** (M = Fe, Ru, Os) and Diradicals **2** (M = Fe, Ru) in the UV/vis Range[a]

compd	λ_1	λ_2	λ_3
1 (M = Fe)	294 (4.1)	463 (2.8)	638 (2.9)
	315 (4.0)		685 (2.9)
	368 (3.9)		
1 (M = Ru)	263 (4.1)		604 (1.5)
	346 (4.0)		661 (2.9)
1 (M = Os)	246 (3.7)		604 (2.6)
	342 (3.8)		657 (2.7)
2 (M = Fe)	314 (4.3)	477 (3.0)	637 (3.1)
	371 (3.9)		686 (3.1)
2 (M = Ru)	263 (4.3)		602 (3.3)
	348 (4.3)		656 (3.3)

[a] λ_1: α-Nitronyl aminoxyl type bands at short wavelengths. λ_2: Metallocene bands. λ_3: α-Nitronyl aminoxyl bands at long wavelengths. Molar extinction coefficients (in L mol^{-1} cm^{-1}) for such absorption maxima are given in parentheses as log ϵ.

Table 6. Formal Half-Wave Potentials (in mV) vs Ag/AgCl for Some of the Studied α-Nitronyl Aminoxyl Radicals Measured in Acetonitrile Solutions at 20 mV/s

compd	$E^{\circ,0/+}$	ΔE_p	$E^{\circ,+/2+}$	E°_p	$E^{\circ,0/-}$	ΔE_p
1 (M = Fe)	+587	80	+917	149	*a*	
1 (M = Ru)	+664	78	*a*		−978	283
2 (M = Fe)	+617	75	+825	95	*a*	
2 (M = Ru)	+646	87	+801	132	*a*	
5 (HNN)	+765	100			−825	160
6 (PHNN)	+753	68			−849	232
ferrocene	+420	86				

[a] Appears as a strongly irreversible process.

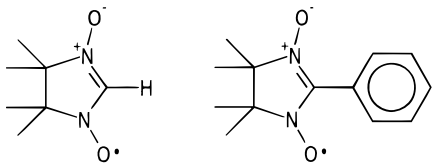

5 **6**

Before the monoradicals **1** (M = Fe, Ru) and diradicals **2** (M = Fe, Ru) were studied by cyclic voltammetry, the voltammograms of two α-nitronyl aminoxyl radicals, one without any substituent at the α position, radical **5**, and the other with a phenyl substituent showing π-conjugation, radical **6**, were recorded as reference compounds. Table 6 summarizes the electrochemical data obtained with all of the radicals studied.

Radical **5** displays two electrochemical processes (Figure 3a): a quasi reversible oxidation process at +765 mV and a reduction process at −825 mV which shows a lower degree of chemical reversibility. Radical **6**, has a similar behavior although it is easier to oxidize and slightly more difficult to reduce due to the presence of π-conjugation with the phenyl substituent.[29]

The cyclic voltammetric response of **1** (M = Fe) (Figure 3b) shows two consecutive one-electron-oxidation processes and a strongly irreversible reduction wave at high negative potential

(29) The departure for the oxidation process of ΔE_p from the constant value of 59 mV expected for an electrochemically reversible one-electron transfer is due to experimental factors, since the value of the reversible one-electron oxidation of ferrocene under the same experimental conditions is very similar. See also: Brown, E. R.: Sandifer, J. R. In *Physical Methods of Chemistry. Electrochemical Methods*; Rossiter, B. W., Hamilton, J. F., Eds.; Wiley: New York, 1986; Vol. 2.

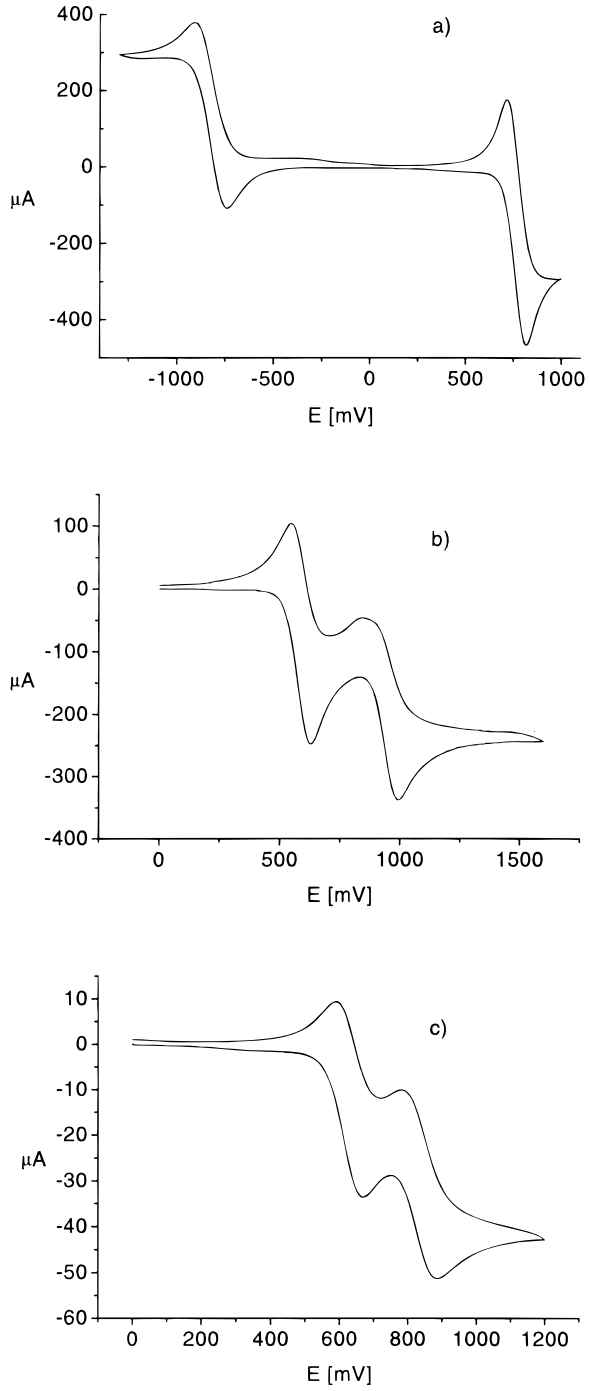

Figure 3. Cyclic voltammograms recorded in an CH_3CN solution containing NBu_4PF_6 (0.1 mol dm^{-3}) of radical **5** (a), monoradical **1** (M = Fe) (b), and **2** (M = Fe) (c).

values. The reversible process at +587 mV arises from the oxidation of the ferrocene unit.[30] The second oxidation process, occurring at +917 mV, exhibits a lower degree of reversibility and is ascribed to the oxidation of the α-nitronyl aminoxyl moiety. The fact that the first oxidation process in **1** (M = Fe) appears at a higher potential value than the oxidation process of the unsubstituted ferrocene (+420 mV) is direct evidence of an electronic interaction between the radical and the ferrocene units, showing at the same time the electron-withdrawing character,[31,32] of the α-nitronyl aminoxyl moiety.

The cyclic voltammetry of radical **1** (M = Ru) shows only one oxidation process with reversible features at +664 mV along with an irreversible reduction process at −978 mV. Both processes arise from the α-nitronyl aminoxyl group.[33] This assignment has been confirmed by a controlled potential coulometry experiment combined with EPR measurements: during the oxidation corresponding to the first anodic process, the signal intensity of the radical moiety rapidly decreases. In addition, further oxidation of radical **1** (M = Ru) shows strongly irreversible features, as can be expected from the oxidation of the ruthenocene moiety, since it is known to be unstable.[33,34]

The cyclic voltammetry of diradicals **2** (M = Fe, Ru) (Figure 3c) presents two quasi-reversible oxidation processes (see Table 6). The first oxidation process in **2** (M = Fe) was assigned, as in the monoradical, to the oxidation of the ferrocene unit of the molecule. It appears at a higher potential value (+617 mV) than the oxidation process in **1** (M = Fe), thus confirming the trend previously observed that the attachment to a ferrocene of an α-nitronyl aminoxyl radical, which has electron-withdrawing character, increases the oxidation potential. The second one-electron-oxidation process in **2** (M = Fe) (+825 mV) corresponds to the oxidation of one of its radical subunits. The oxidation of the second radical subunit that would yield a tricationic species appears at a very high oxidizing potential as a highly irreversible process, probably due to the instability of the resulting charged species. Similarly, the ruthenocene diradical **2** (M = Ru) shows two quasi-reversible oxidation processes at +646 and +801 mV, respectively. In contrast to what is observed for the monoradical counterpart, the second oxidation process for diradical **2** (M = Ru) does not appear as a highly irreversible process. Thus, for the same reasons as in **1** (M = Ru), both oxidation processes may be ascribed to the radical subunits. As occurs in **2** (M = Fe), further oxidation to a trication takes place in **2** (M = Ru) only at very high oxidizing potentials and is strongly irreversible. The most relevant aspect of the cyclic voltammetry of diradicals **2** (M = Fe, Ru) is the fact that the oxidation processes of both radical subunits appear separated at different potentials and not as a two-electron process at a certain potential. This result clearly confirms the presence of an electronic interaction between both α-nitronyl aminoxyl radical centers.

ESR spectroscopy provides more detailed information about the electronic structure of systems with unpaired electrons, as in **1** and **2**, as well as of the intramolecular interactions in these compounds.[35] The ESR spectra of radicals **1** (M = Fe, Ru, Os) under isotropic conditions, where the molecules are freely tumbling, gave the isotropic g values (g_{iso}) and the isotropic

(30) Indeed, a controlled potential coulometry experiment (performed at +750 mV) that consumed one electron per molecule turned the original reddish-brown solution to a deep green color, which is typical of oxidized ferrocenium species. (Duggan, D. M.; Hendrickson, D. N. *Inorg. Chem.* **1975**, *14*, 955−970.) Accordingly, the EPR spectrum of the oxidized species keeps the characteristic five-line pattern of an α-nitronyl aminoxyl radical, with a shift in the g value (g = 2.0065).

(31) Kuwana, T.; Bublitz, D. E.; Hoh, G. *J. Am. Chem. Soc.* **1960**, *82*, 5811.

(32) Gubin, S. P.; Smirnova, S. A.; Denisovich, L. I.; Lubovich, A. A. *J. Organomet. Chem.* **1971**, *30*, 243−255.

(33) Although the electrochemistry of substituted ruthenocenes is more complex and less well understood than that of ferrocenes, the first oxidation step may be more reasonably ascribed in this case to the oxidation of the radical part of the molecule, since the oxidation of unsubstituted ruthenocene has been reported to appear as a highly irreversible process at higher oxidizing potentials. See also refs 28, 29, and the following: Denisovitch, L. I.; Zakurin, N. V.; Bezrukova, A. A.; Gubin, S. P. *J. Organomet. Chem.* **1974**, *81*, 207. Gale, R. J.; Job, R. *Inorg. Chem.* **1981**, *20*, 42−45. Hill, M. G.; Lamanna, W. M.; Mann, K. R. *Inorg. Chem.* **1991**, *30*, 4690−4692.

(34) Elschenbroich, C.; Salzer, A. *Organometallics*; VCH Publishers: Weinheim, 1992; p 330.

Table 7. Isotropic g Factors and Hyperfine Coupling Constants (in mT) for Radicals **1** (M = Fe, Ru, Os) Obtained by Computer Simulation of the ESR Spectra in Toluene/$CHCl_3$ (4:1) Solutions at 300 K

compd	g_{iso}[a]	N ($I = 1$)[b]	H ($I = 1/2$)[c]	M (I)[d]
1 (M = Fe)	2.0056	0.752	0.021	^{57}Fe ($I = 1/2$): 0.260
1 (M = Ru)	2.0057	0.752	0.021	^{101}Ru ($I = 5/2$): 0.06
				^{99}Ru ($I = 5/2$): 0.053
1 (M = Os)	2.0049	0.751	0.020	*e*
5 (PHNN)	2.0065	0.750	0.021	
6 (HNN)	2.0062	0.722	0.020	

[a] Estimated precision of g_{iso} values is below $\pm 10^{-4}$. [b] Coupling with two equivalent N atoms. [c] Coupling with 12 equivalent hydrogen atoms of the four CH_3 groups. [d] Coupling with one metal nucleus of the metallocene unit. [e] The coupling with the Os nucleus is not observed because of a large quadrupolar relaxation phenomenon. See ref 35.

hyperfine coupling constants of the unpaired electron of the molecules with the different nuclei with nonzero magnetic moments (a_i). Five main groups of lines (Table 7) are observed with relative intensities of 1:2:3:2:1 resulting from the coupling of the unpaired electron with two equivalent nitrogen nuclei ($I = 1$).[10] These five groups of lines show a complex shape of overlapping signals arising from additional couplings with 12 equivalent hydrogen atoms of the four methyl groups (Figure 4).

No significant couplings with the protons of the cyclopentadienyl rings are produced, in accordance with the fact that the spin density on the substituents linked to the α-carbon atom of this kind of radical is always very small because the SOMO orbital has a node on this carbon atom and the spin density on these substituents is transmitted mainly by a spin polarization mechanism. This mechanism is operative regardless of whether the substituent at the α-position is rotating freely under isotropic conditions, and consequently the spectra must not show any significant change with the temperature, as it is indeed experimentally observed. Despite the low spin density on the metallocene units of radicals **1** (M = Fe, Ru, Os), the large nuclear magnetic moments of the metal nuclei having magnetically active isotopes ($I \neq 0$)[36] make possible the direct observation of their coupling with the unpaired electron for the ferrocene and ruthenocene radicals as a set of low-intensity satellite lines beside each of the five main groups of lines.[37,38]

The computer simulation of the ESR spectra of radicals **1** (M = Fe, Ru, Os) under isotropic conditions yields the hyperfine coupling constants summarized in Table 7. For all of these metallocene monoradicals the values of the coupling constants with the two equivalent nitrogen atoms and the 12 equivalent methyl hydrogen atoms are practically coincident, and very similar to those exhibited by other substituted α-nitronyl aminoxyl radicals.[10] Therefore, the unpaired electron of metallocene radicals **1**, when these species are freely tumbling in solution, is mainly distributed on both NO groups, with a very small spin density on the metallocene subunits.

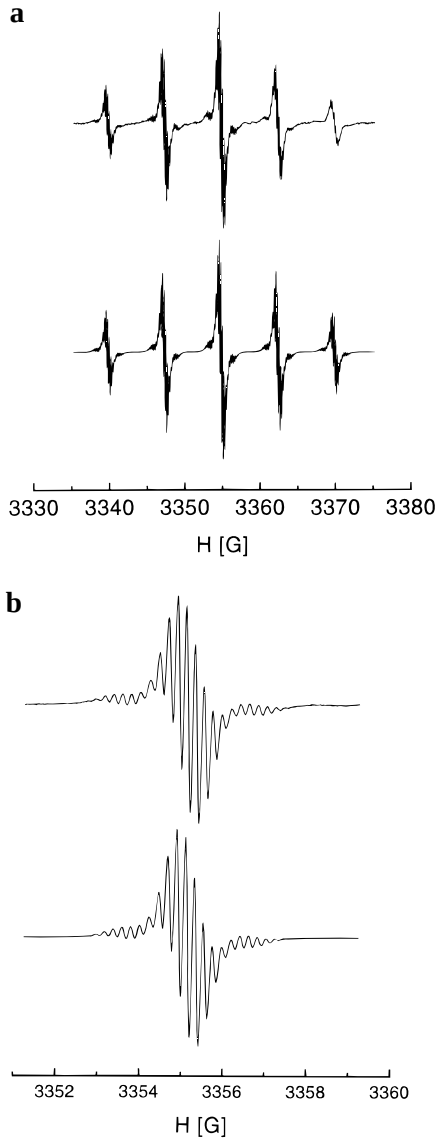

Figure 4. (a) ESR spectrum of radical **1** (M = Ru) in toluene at 300 K under isotropic conditions. (b) Enlarged central group of lines of radical **1** (M = Ru) in toluene at 300 K. Experimental (upper) and simulated (lower) spectra.

The presence of spin density on the metal atoms of radicals **1** (M = Fe, Ru, Os) was also confirmed by means of their ESR spectra in frozen solution. These spectra (Figure 5) have all of the typical singularities—steps and divergencies—of an α-nitronyl aminoxyl radical due to the magnetic anisotropies of the **g** and **A** tensors.[10]

The principal components of the **g** and **A** tensors (Table 8) were obtained by computer simulation. As expected, the averaged principal components, g_{av}, for radicals **1** (M = Fe, Ru, Os) and **6** are in good agreement with the isotropic g values (Table 7) measured under isotropic conditions. Comparing the values of the principal components of radical **6** with those of radicals **1** (M = Fe, Ru, Os), one can observe that some of the values of the latter, as well as their g_{iso} values, are slightly lower, the negative shift being larger for the osmocene derivative. There are three different terms contributing to shift the value of each particular g component of the **g** tensor with respect to the g

(35) Weil, J. A.; Bolton, R. B.; Wertz, J. E. *Electron Paramagnetic Resonance*; John Wiley & Sons: New York, 1994.
(36) Solodovnikov, S. P.; Kreindlin, A. Z.; Shilovsteva, L. S.; Rybinskaya, M. I. *Metalloorg. Khim.* **1991**, *4* (2), 311−315.
(37) Although the hyperfine coupling constant and therefore the spin density for the ruthenocene radical are both lower than for the ferrocene derivative, the satellite lines observed for radical **1** (M = Ru) are more intense than those in the spectrum of **1** (M = Fe). This is merely a consequence of the higher natural isotopic abundance of the nucleus of ruthenium which gives rise to the hyperfine coupling (17% for ^{101}Ru, $I = 5/2$, and 12.7% for ^{99}Ru, $I = 5/2$) than in the iron case (2.64% ^{57}Fe, $I = 1/2$).
(38) Surprisingly the osmocene radical **1** (M = Os) does not show any satellite lines despite having two isotopes with nonzero nuclear magnetic moment and large enough natural abundance to be observed (1.64% for ^{187}Os, $I = 1/2$, and 16.1% for ^{189}Os, $I = 3/2$). This result can be ascribed to an efficient quadrupolar relaxation phenomenon that takes place during the ESR experiment because of the large quadrupolar moment of the heavy element osmium.[35]

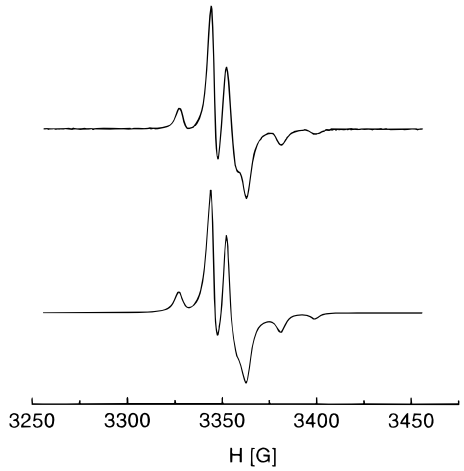

Figure 5. Upper: experimental ESR spectrum of **1** (M = Ru) in frozen toluene/$CHCl_3$ (4:1) at 160 K. Lower: simulated spectrum using the data given in Table 8.

Table 8. Principal Components of **g** and **A** Tensors (in mT) for Monoradicals **1** (M = Fe, Ru, Os) and **6** and Diradicals **2** (M = Fe, Ru) Obtained by Simulation of the ESR Spectra in Frozen Solutions

compd	g_x	g_y	g_z	g_{av}[c]	A_{xx}	A_{yy}	A_{zz}
1 (M = Fe)[a]	2.0009	2.0065	2.0095	2.0056	1.90	0.15	0.15
1 (M = Ru)[a]	2.0006	2.0060	2.0095	2.0054	1.90	0.15	0.15
1 (M = Os)[a]	1.9976	2.0085	2.0085	2.0049	1.92	0.15	0.15
6 (PHNN)[a]	2.0018	2.0070	2.0110	2.0066	1.90	0.15	0.15
2 (M = Fe)[b]	1.996	2.002	2.014	2.004	0.90	0.075	0.075
2 (M = Ru)[b]	1.987	2.006	2.016	2.003	0.90	0.075	0.075

[a] Determined by the simulation of signals corresponding to the $\Delta m_s = \pm 1$ transition. The principal g components were determined with an estimated precision of $\pm 5 \times 10^{-4}$. [b] Determined by simulation of the signals corresponding to the forbidden $\Delta m_s = \pm 2$ transition using the perturbation theory up to the second-order approximation. The principal g components in such simulations were obtained with an estimated precision of $\pm 10^{-3}$. [c] Averaged g factors were calculated using $g_{av} = (g_x + g_y + g_z)/3$.

value of the free electron. These are: the relativistic mass correction of the Zeeman energy, the coupling of the electron spin with diamagnetic currents induced by a magnetic field, and finally, the spin−orbit coupling term.[39] Considering that the relativistic term is the same for all radicals studied, the observed negative shifts in the principal components of **1** (M = Fe, Ru, Os) may arise either from diamagnetic currents induced on the five-membered rings or from a spin−orbit coupling.[40] The observed negative shifts of the **g**-tensor elements in radicals **1** (M = Fe, Ru, Os) could basically arise from a spin−orbit coupling (diamagnetic currents generally cause a positive shift) in which the metal atoms of the metallocene units play an important role. Indirectly, this result indicates that in the osmocene radical **1** (M = Os) the osmium atom also carries a certain spin density as occurs for the other two metallocene radicals.

Therefore, from the ESR measurements of monoradicals **1** (M = Fe, Ru, Os) it is possible to conclude that the metal atoms of the metallocene units have a nonvanishing spin density and are bridges able to transmit a small spin density through them, hence coupling magnetically two radical centers when they are connected to the two Cp rings. The mechanism through which this small spin density appears on the metal nuclei is different depending on the experimental conditions and on the conformation of the free radical. Under isotropic conditions, where the α-nitronyl aminoxyl units are freely rotating, it seems that the spin polarization through covalent bonds could be the dominant mechanism, while for frozen conformations a direct overlap between the radical unit and the d orbitals of the metal is also involved.

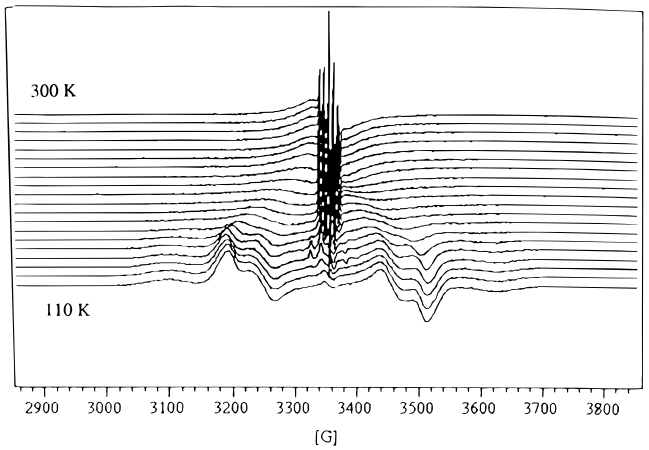

Figure 6. Temperature dependence of ESR spectra of diradical **2** (M = Fe) in toluene/$CHCl_3$ (4:1) in the temperature range 110−300 K.

The ESR spectra of diradicals **2** (M = Fe, Ru) in isotropic solutions at room temperature consist of an overlap of two types of spectra: a broad intense single line with a large peak-to-peak width of ca. 6.4 mT, assigned to the diradical molecules having a large spin−spin dipolar interaction which is not completely averaged out by the molecular tumbling, and a set of five narrower lines exhibiting a hyperfine coupling with two equivalent nitrogen nuclei ($a_N = 0.75$ mT). The latter signals amount to less than 1% of the total signal intensity showing the typical hyperfine coupling constant of an α-nitronyl aminoxyl radical and arise from adventitious monoradicals.

The temperature dependence (110−300 K) of the ESR spectra (Figure 6) of diradical **2** (M = Fe) exhibits the characteristic features of a dynamic behavior of the ESR fine structure for a triplet species under reorientational motions.[41] Thus, the spectra in frozen solutions (i.e., below 160 K) have the typical pattern of a rigid distribution of randomly oriented triplets with nonaxial symmetries. By the simulation of the spectra of diradicals **2** (M = Fe, Ru) under such conditions (Figure 7) the zero-field-splitting (zfs) values of both triplets were determined to be $D' = 26$ mT and $E' = 1.6$ mT for **2** (M = Fe), and $D' = 34.0$ mT and $E' = 9.0$ mT for **2** (M = Ru).

The spectra of both triplets change progressively as the frozen glassy solutions soften and molecules start to reorient. Thus, in viscous solutions, typically between 170 and 230 K, where the reorientational motion of triplets is very low, the ESR steps and divergencies are broadened and shifted toward the central region, so that the spectrum consists of two highly asymmetrically broadened lines. When the reorientational motion becomes faster (i.e., in fluid solutions at temperatures higher than 230 K), the two lines collapse into one broad line that shows a narrowing process when the temperature is further increased. Even at the highest temperature assayed (370 K) the reorientational rate is not high enough for achieving a complete motional averaging of the spin−spin dipolar interaction so that it is not possible to observe the isotropic hyperfine coupling with the four nitrogen atoms for the triplets **2** (M = Fe, Ru).

For molecular triplets where the contribution to the zfs from the spin−orbit coupling is small, the D' and E' parameters can

(39) Un, S.; Atta, M.; Fontecave, M.; Rutherford, W. *J. Am. Chem. Soc.* **1995**, *117*, 10713−10719 and references therein.
(40) Stone, A. J. *Mol. Phys.* **1963**, *6*, 509−515.
(41) Lee, S.; Brown, I. M.. *Phys. Rev. B* **1986**, *34*, 1442−1448.

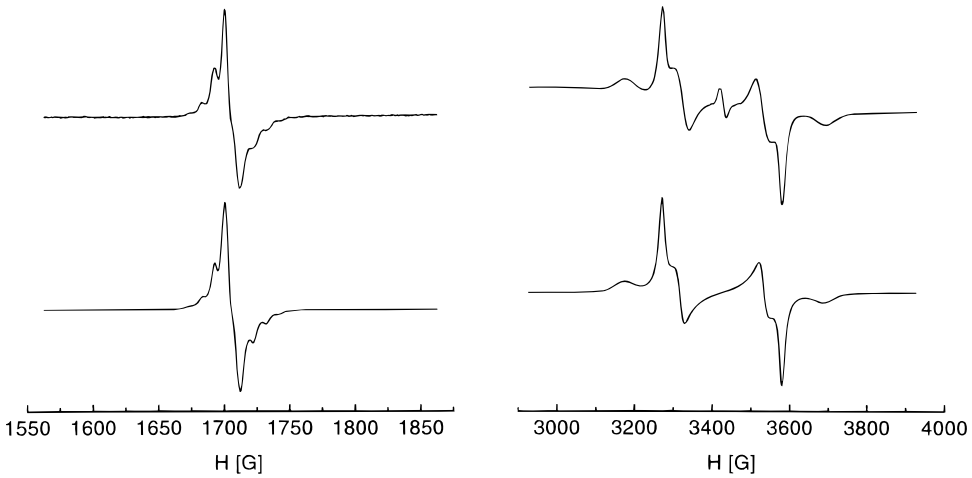

Figure 7. ESR spectra of diradical **2** (M = Fe) in toluene/$CHCl_3$ (4:1) at 29 K. Left: Signals corresponding to $\Delta m_s = \pm 2$ forbidden transition. Right: Signals corresponding to $\Delta m_s = \pm 1$ transition. Top: experimental spectra. Bottom: simulated spectra using the principal components of the **g** and **A** tensors shown in Table 8 and the zfs parameters quoted in text.

be described by the spin−spin dipolar interaction.[42] In such molecular systems the zfs parameters depend critically on the distribution of the unpaired spins and the interatomic separations. The D' parameter is the most sensitive to the mean distance between atoms having large spin densities while E' is related to the molecular symmetry. Consequently, the experimental zfs parameters of a triplet can be used to estimate its molecular conformation, assuming that the spin−orbit coupling is insignificant and the two electrons have a fixed and known distribution in the molecule. The spin-density distribution in substituted α-nitronyl aminoxyl radicals remains nearly constant regardless of the substituent being mainly localized on the five atoms of the O−N−C−N−O groups. Therefore, the spin-density distribution on each of the two radical subunits of **2** can be assumed to be similar to that of radical **6** obtained by semiempirical AM1 calculations.[43]

To estimate the molecular conformation of diradicals **2** (M = Fe, Ru) in frozen solution we used a program which calculated the theoretical D' and E' parameters expected for a given relative arrangement of two α-nitronyl aminoxyl units. To reproduce the experimental D' and E' values for diradical **2** (M = Fe) we had to use a molecular conformation with only one imidazoline ring keeping planarity with its adjacent cyclopentadienyl ring, i.e., $\phi_1 = 0 \pm 10°$, while the other imidazoline ring is tilted by an angle ϕ_2 of $30 \pm 10°$. Moreover, the molecule must be in a *cisoid* conformation defined by an angle φ of $60 \pm 10°$.[44] This conformation is strikingly similar, although not identical, to that previously described for the solid state structure of **2** (M = Fe), with $\phi_1 = 7°$, $\phi_2 = 24°$, and $\varphi = 73°$. The maintenance in a frozen solution of the intramolecular hydrogen bond, observed in the solid state, may be the cause of this similarity. To reproduce the experimental D' and E' of **2** (M = Ru) we had to use a conformation similar to that in **2** (M = Fe), but with a φ angle of $50 \pm 10°$. Thus, this diradical seems to keep the molecular conformation tethered by an intramolecular hydrogen bond. In this diradical the hydrogen bond forces a slightly lower φ angle than in **2** (M = Fe), probably because of the larger separation between the two cyclopentadienyl rings in the ruthenocene (3.61 Å)[21] than in the ferrocene moiety (3.30 Å).[34]

ESR spectra of diradicals **2** (M = Fe, Ru) in rigid glassy solutions also show the forbidden $\Delta m_s = \pm 2$ transition signals which appear at the half magnetic field region as structured signals due to the hyperfine coupling with the nitrogen nuclei. Such signals can be nicely simulated (Figure 7) by using the principal values of the **g** and **A** tensors, Table 8. Due to the large spin−spin dipolar interaction in both diradicals **2** (M = Fe, Ru), the simulation of the signals corresponding to the forbidden $\Delta m_s = \pm 2$ transition had to be performed taking into account the second-order term in the perturbation theory treatment of fine structure.[45,46] As in the case of the metallocene monoradicals, the g_{av} factors of **2** (M = Fe, Ru) are lower than that of monoradical **6**. Again, the presence of a small spin−orbit coupling may cause this negative shift in the diradicals. The principal components of the **A** tensor of diradicals **2** (M = Fe, Ru), shown in Table 8, are interestingly half of those shown by the corresponding monoradicals **1** (M = Fe, Ru), indicating that both diradicals have a strong magnetic exchange interaction, J_{intra}, which overcomes the magnitudes of the hyperfine coupling constants; i.e., $J_{intra} \gg a_N$.

To determine the ground state multiplicity and the singlet−triplet separation, $2J_{intra}$, of diradicals **2** (M = Fe, Ru), the temperature dependence of the $\Delta m_s = \pm 2$ signals was studied. As the intensity of the signals of both diradicals dramatically decreases at temperatures below 25 K (Figure 8), we concluded that the singlet is the ground state, the magnetic interaction

(42) The dipolar interaction is given by eqs 1 and 2, in which the angular

$$D' = {}^3/_4 g^2\beta^2\langle\Phi_1|1/r^3 - 3z^2/r^5|\Phi_2\rangle \quad (1)$$

$$E' = {}^3/_4 g^2\beta^2\langle\Phi_1|(y^2 - x^2)/r^5|\Phi_2\rangle \quad (2)$$

brackets imply an average over the spatial wave function of the two electrons, $\Phi_{1,2}$, r is the distance between them, and x, y, and z are the components of the distance vector. See also: Wasserman, E.; Snyder, L. C.; Yager, W. A. *J. Chem. Phys.* **1964**, *41*, 1763.

(43) This spin density distribution is in accordance with experimental data obtained by ESR and NMR spectroscopic measurements and also by polarized neutron diffraction experiments. See: Davis, M. S.; Morokuma, K.; Kreilick, R. W. *J. Am. Chem. Soc.* **1972**, *94*, 5588−5592. Neely, J. W.; Hatch, G. F.; Kreilick, R. W. *J. Am. Chem. Soc.* **1974**, *96*, 652−656. Zhedulev, A.; Barone, V.; Bonnet, M.; Delley, B.; Grand, A.; Ressouche, E.; Rey, P.; Subra, R.; Schweizer, J. *J. Am. Chem. Soc.* **1994**, *116*, 2019−2027. Zhedulev, A.; Ressouche, E.; Schweizer, J.; Turek, P.; Wan, M.; Wang, H. *J. Magn. Magn. Mater.* **1995**, *144*, 1441−1442.

(44) The variance of the zfs parameters within the given ±10° intervals is very large, i.e., 20% for D' and 53% for E' in **2** (M = Fe), and 7% for D' and 60% for E' in **2** (M = Ru), giving an idea of the precision of this structural assignment.

(45) Teki, Y.; Takui, T.; Itoh, K. *J. Chem. Phys.* **1988**, *88*, 6134.

(46) For such a simulation it was assumed that the **g** and **D** tensors are collinear for diradicals **2** (M = Fe, Ru).

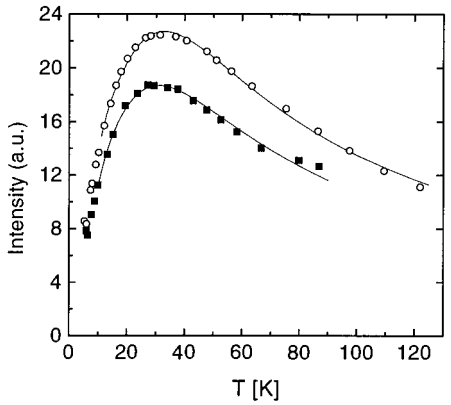

Figure 8. Temperature dependence of the intensity of the $\Delta m_s = \pm 2$ signals of diradicals **2** (M = Fe) (circles) and **2** (M = Ru) (squares). Continuous lines are the fits of experimental data to the Bleaney−Bowers equation.

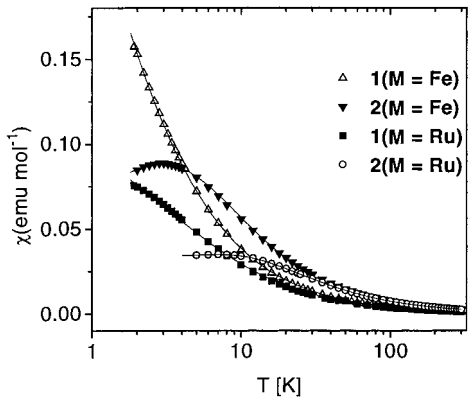

Figure 9. Temperature dependence of the molar paramagnetic susceptibility, χ, of monoradicals **1** (M = Fe, Ru) and diradicals **2** (M = Fe, Ru). The solid lines represent the fits of experimental data: Bleaney−Bowers equation for radicals **1** (M = Fe, Ru) and eq 4, corresponding to a dimer of dimers model, for diradicals **2** (M = Fe, Ru).

between the two radical moieties being antiferromagnetic. The intensity data of $\Delta m_s = \pm 2$ signals were fitted to the Bleaney−Bowers equation (eq 3), used for describing the magnetic

$$IT = C/(3 + e^{-2J/kT}) \qquad (3)$$

behavior of dimers,[47] yielding a magnetic exchange constant of $J/k_B = -29$ K for diradical **2** (M = Fe) and $J/k_B = -27$ K for diradical **2** (M = Ru).[48]

Solid State Magnetic Properties of Metallocene Radicals. DC magnetic susceptibility measurements of radicals **1** (M = Fe, Ru) (Figure 9) show quasi-paramagnetic behaviors which can be fitted to the Curie−Weiss law [Weiss constants of $\theta = -0.7$ K for **1** (M = Fe) and −3.0 K for **1** (M = Ru)], indicating the existence of very weak antiferromagnetic intermolecular interactions in both monoradicals. The fitting of the experimental data can be considerably improved by using the Bleaney−Bowers equation[47] with a magnetic exchange interaction of $J/k_B = -0.8$ K for **1** (M = Fe) and $J/k_B = -0.7$ K for **1** (M = Ru).[49]

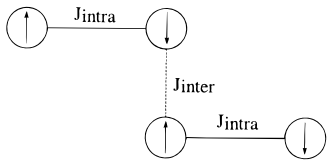

Figure 10. Schematic representation of the magnetic model of a dimer of dimers used to fit experimental data for **2** (M = Fe, Ru).

Table 9. Summary of Intra- and Intermolecular Exchange Constants (in K) Obtained for Crystalline Radicals **2** (M = Fe, Ru) by Fitting the Model Described in the Text to the Experimental Magnetic Susceptibility Data

compd	J_{intra}/k_B	J_{inter}/k_B
2 (M = Fe)	−3.2	−4.2
2 (M = Ru)	−8.8	−12.3

The last magnetic model is more in accordance with the observed crystal packing, which shows clearly the presence of dimers linked by two complementary hydrogen bonds. According to the so-called McConnell I mechanism, intermolecular magnetic interactions can be rationalized by analyzing the overlap of atomic orbitals belonging to atoms with large spin densities.[50] Dominant contacts of atoms of two neighboring radical centers with spin densities having the same sign produce antiferromagnetic interactions while those having opposite signs yield ferromagnetic interactions. In the case of α-nitronyl aminoxyl radicals, a direct contact between N−O units, which carry most of the spin density, determines an antiferromagnetic coupling. The shortest distance between N−O groups in **1** (M = Fe), N2−O2···O2^i−N2^i [$i = 2 - x, 2 - y, 1 - z$; d(O2···O2^i) = 4.41 Å], occurs among the molecules arranged in a dimer geometry through two complementary hydrogen bonds. Thus, the large distance between the interacting N−O groups as well as their relative arrangement explain the antiferromagnetic nature and the weakness of the observed magnetic interaction.

The magnetic susceptibility data (Figure 9) for diradicals **2** (M = Fe) and **2** (M = Ru) exhibit broad maxima at 3 and 9 K, respectively, suggesting an analogous low-dimensional antiferromagnetic behavior. Attempts to fit these experimental data to a Bleaney−Bowers equation (eq 3), as in frozen solution, were unsuccessful. Therefore, the data were fitted to a magnetic model, based on dimers but having an additional exchange interaction consistent with the crystalline structure of **2** (M = Fe) (see below), that describes the magnetic behavior of a dimer of dimers (eq 4), a four spin cluster model (Figure 10)[51] where J_{intra}/k_B represents the intradimer exchange constant and J_{inter}/k_B the exchange constant between two radicals of neighboring dimers, E_i are the energies of the different possible states of

(47) Carlin, R. L. *Magnetochemistry*; Springer-Verlag: Berlin, 1986; pp 71−77.

(48) The intensity data below 10 K of both diradicals showed a larger intensity than that predicted by the Bleaney−Bowers equation. This could be ascribed to the presence of small amounts of molecules in different conformations that have weaker antiferromagnetic interactions (or even ferromagnetic interactions) between the radical centers than the most predominant conformation. These minor conformations must contribute significantly to the $\Delta m_s = \pm 2$ signal at low temperatures since the signal of the predominating conformer with strong antiferromagnetic interactions becomes weaker.

(49) The fitting of the experimental data of **1** (M = Ru) was improved if the Bleaney−Bowers equation was corrected in order to take into account interactions between magnetic dimers by a mean field treatment. This correction was performed by using an effective temperature $T_{eff} = T - \theta$. See: Carlin, R. L. *Magnetochemistry*; Springer-Verlag: Berlin, 1986; p 88.

(50) (a) McConnell, H. M. *J. Chem. Phys.* **1963**, *39*, 1910. (b) Goodenough, J. B. *Magnetism and the Chemical Bond*; Interscience: New York, 1963; p 163. (c) McConnell, M. H. *Proc. Robert A. Welch Found. Conf. Chem. Res.* **1967**, *11th*, 144.

(51) Shiomi, D.; Tamura, M.; Sawa, H.; Kato, R.; Kinoshita, M. *J. Phys. Soc. Jpn.* **1993**, *62*, 289.

the diradicals, and $A = 2Ng^2\mu_B{}^2/3nk_B$ with n the number of spins in the cluster (the other constants have the usual meaning).

$$\chi T = \frac{A\sum_i [S_i(S_i+1)(2S_i+1)e^{-E_i/k_BT}]}{\sum_i [(2S_i+1)e^{-E_i/k_BT}]} \quad (4)$$

$$E_1 = J_{intra} + J_{inter}/2 - (4J_{intra}{}^2 - 2J_{intra}J_{inter} + J_{inter}{}^2)^{1/2} \qquad S_1 = 0$$

$$E_2 = J_{intra} + J_{inter}/2 + (4J_{intra}{}^2 - 2J_{intra}J_{inter} + J_{inter}{}^2)^{1/2} \qquad S_2 = 0$$

$$E_3 = J_{inter}/2 - (J_{intra}{}^2 + J_{inter}{}^2)^{1/2} \qquad S_3 = 1$$

$$E_4 = J_{inter}/2 - (J_{intra}{}^2 + J_{inter}{}^2)^{1/2} \qquad S_4 = 1$$

$$E_5 = J_{intra} - J_{inter}/2 \qquad S_5 = 1$$

$$E_6 = -J_{intra} - J_{inter}/2 \qquad S_6 = 2$$

This magnetic model is consistent with the molecular arrangement observed in the solid state since the molecule adopts a particular conformation, determined by an intramolecular C_{methyl}−H01A···O2−N2 hydrogen bond, resulting in a short O2···N4 distance [d(O2···N4) = 3.67 Å]. This relative arrangement of the two radical subunits of **2** (M = Fe) is responsible for the intramolecular magnetic interaction J_{intra}. On the other hand, the shortest distance between N−O units of different molecules occurs also in a dimer fashion, O2···N2^i [$i = 2 - x, -y, 2 - z$; d(O2···N2^i) = 4.43 Å] and causes the pairwise interaction between dimers with a magnetic interaction J_{inter}.

Table 9 summarizes the exchange coupling constants obtained by fitting the experimental data to this four spin cluster magnetic model. Remarkable are the small intradimer exchange constants J_{intra}/k_B obtained for both diradicals **2** (M = Fe, Ru) in the solid state which are clearly lower than those found in frozen solution by ESR. Such a discrepancy may be ascribed either to small differences in the molecular conformation adopted by the molecules in the solid state and in frozen solutions or to a slight spin density redistribution in the solid state due to the close packing of the molecules.

It is already known that, in some highly localized diradicals in which coexist a through-space with a through-bond pathway for the magnetic interactions, small changes of their molecular geometry produce significant changes on the intramolecular exchange coupling constant.[2d] Therefore, the observed difference in the magnetic behaviors of **2** (M = Fe, Ru) in the solid state and in frozen solution suggest the presence of a direct through-space interaction between the two SOMOs of the two radical units along with the magnetic interaction produced via spin polarization through the σ bonds of the metallocene coupler unit.

Conclusions

The results obtained with monoradicals **1** (M = Fe, Ru, Os) and diradicals **2** (M = Fe, Ru) show that metallocenes are effective magnetic couplers that transmit the magnetic interaction through their σ skeleton, via a spin polarization mechanism, and also favor, under proper circumstances, a direct overlap between the SOMOs of the two radical units. The combination of both mechanisms leads to the appearance of an antiferromagnetic interaction that is very sensitive to the molecular conformation.

Acknowledgment. This work was financially supported by the DGCYT (PB96-0872-C02-01), the Generalitat de Catalunya (Grant, SGR 95-00507), and the Human Capital and Mobility Program of EU (Network: ERB CHRXCT 940538). O.J. thanks the Generalitat de Catalunya for the award of a doctoral fellowship.

Supporting Information Available: Tables of structure solution and refinement data (S1 and S2), hydrogen atom coordinates (S3 and S4), bond lengths and angles (S5 and S6), and anisotropic thermal paramenters (S7 and S8) for the structures reported (14 pages). Ordering information is given on any current masthead page.

IC980495H